Electrochemical Oxidation of Molybdenum Metal in 0.5 M H_2SO_4 Studied by Core and Valence Band X-ray Photoelectron Spectroscopy and Interpreted by Band Structure Calculations

Holly Hixson and Peter M. A. Sherwood*

Department of Chemistry, 111 Willard Hall, Kansas State University, Manhattan, Kansas 66506-3701

Received March 12, 1996. Revised Manuscript Received July 8, 1996[⊗]

The behavior of molybdenum metal in 0.5 M sulfuric acid treated at various potentials has been studied using core and valence band X-ray photoelectron spectroscopy in a previously described anaerobic cell. Valence band spectra of molybdenum and its oxidized species were interpreted by ab initio band structure calculations. The study indicates that Mo(IV) and Mo(VI) (including possibly Mo(V) in some cases) were formed, in a mixed film that included some metal, as the potential of the system was increased within the active range of molybdenum. Three regimes were found. At potentials at or below 0.0 V (*vs* the saturated calomel electrode) the metal remained practically unoxidized. At potentials between 0.5 and 2.0 V about 75% of the mixed film consisted of oxidized molybdenum with the predominant oxide being Mo(IV). When the polarization time at 2.0 V increased the mixed film continued to consist of about 80% of oxidized molybdenum, but the predominant oxide was Mo(V/VI), and the film became mechanically unstable, eventually falling off the metal.

Introduction

The oxidation behavior of molybdenum metal in sulfuric and hydrochloric acid has been studied using various techniques such as cyclic voltammetry[1−7] and X-ray photoelectron spectroscopy (XPS).[8−13] Molybdenum has been shown to oxidize in the presence of oxygen dissolved in water at rest potential.[14] Molybdenum has been shown to be relatively inert with respect to oxidation and has often been used in the formulation of corrosion-resistant alloys. However, the oxidative behavior of molybdenum needs to be more fully understood in order to maximize its applications.[15]

The previous studies of the behavior of oxide films on molybdenum metal surfaces have used core XPS and various curve-fitting methods to elucidate the oxide composition at various potentials. However, valence band XPS has not been considered in most of these studies. The valence band region in the molybdenum oxidation system can be used in the near Fermi edge region to distinguish between the various molybdenum oxides. This information can be used to complement the information obtained from the core-level spectra, as well as to reveal information that cannot be gained from core spectra alone.[16] The additional use of angle-resolved XPS allows surface and near-surface species to be distinguished, and the anaerobic cell[17] provides a controlled experimental environment.

In this paper we report details of the electrochemical oxidation of molybdenum in sulfuric acid providing a careful analysis of the various oxides present by a combination of angle-resolved core and valence band XPS, with curve fitting used to analyze the former region and calculated spectra used to analyze the latter region. We also discuss the appropriateness of cluster versus band structure models for the interpretation of the valence band regions found in the molybdenum oxidation system. The method of data analysis used in this study has been designed to minimize errors that may be created due to the subjective nature of removing a background from a spectrum prior to fitting of the data. By including the background as part of the fitting process and fitting the original data, one can see how the choice of background influences the fit. When fitting data that has had the background removed, errors in background removal may lead to spectral features that can be fit into new peaks and, hence, might be falsely identified as a chemically important species.

[⊗] Abstract published in *Advance ACS Abstracts,* September 1, 1996.

(1) Hull, M. N. *Electroanal. Chem. Interfac. Chem.* **1972**, *38,* 143.
(2) Kuesner, H. *Z. Electrochem.* **1910**, *16,* 754.
(3) Becker, E.; Hilberg, H. *Z. Electrochem.* **1925,** *31,* 31.
(4) Besson, J.;Drautzberg, G. *Electrochem. Acta* **1960**, *3,* 158.
(5) Wikstrom, L. L.; Nobe, K. *J. Electrochem. Soc.* **1969**, *116,* 525.
(6) Heumann, T.; Hauck, G. *Z. Metallkd.* **1965,** *56,* 75.
(7) Pozdeeva, A. A.; Antonovskaya, E. I.; Sukhotin, A. M. *Corros. Sci.* **1966**, *6,* 149.
(8) Kozhevnikov, V. B.; Tsenta, T. E.; Knyazheva, V. M.; Kolotyrkin, Ya. M. *Prot. Met.* **1983**, *1905,* 569.
(9) Brox, B.; Yi-Hua, W.; Olefjord, I. *J. Electrochem. Soc.: Electrochem. Sci. Technol.* **1988,** *135,* 2184.
(10) Ansell, R. O.; Dickinson, T.; Povey, A. F.; Sherwood, P. M. A. *J. Electroanal. Chem.* **1979**, *98,* 79.
(11) Urgen, M.; Stolz, U.; Kirchheim, R. *Corros. Sci.* **1990**, *30,* 377.
(12) Lu, Y. C.; Clayton, C. R. *Corros. Sci.,* **1989,** *29,* 927.
(13) Povey, A. F.; Metcalfe, A. A. *J. Electroanal. Chem.* **1977**, *84,* 73.
(14) Hixson, H.; Sherwood, P. M. A. *J. Chem. Soc., Faraday Trans.* **1995**, *91,* 3593.
(15) Bonen, D.; Sarkar, S. L. *Proceedings of the Sixteenth International Conference on Cement Microscopy;* Apr 1994.
(16) Sherwood, P. M. A. *J. Vac. Sci. Technol.* **1991**, *A9,* 1493.
(17) Liang, Y.; Paul, D. K.; Xie, Y.; Sherwood, P. M. A. *Anal. Chem.* **1993**, *65,* 2276.

S0897-4756(96)00187-1 CCC: $12.00

Experimental Section

Instrumentation. All XPS spectra were obtained using a VSW HA100 spectrometer with a UHV chamber that has been specifically designed for liquid-exposure experiments without exposure to air.[17] The base pressure of the system is 10^{-10} Torr. Achromic Mg Kα radiation (1253.6 eV with a line width of ca. 0.8 eV), at a power of 275 W (12 kV, 25 mA). All data were recorded in the fixed analyzer transmission (FAT) mode, using a 25 eV pass energy for all core regions and a 50 eV pass energy for all valence-band regions. All data was collected using at least 17 points/eV to ensure identification of subtle features that might be missed at lower resolution. The spectrometer scale was calibrated using copper.[18] The peak positions were adjusted for possible charging according to the C 1s peak (284.6 eV) resulting from small amounts of hydrocarbon on the surface of the sample.

Sample Preparation. Mo foil (99.9+%, 0.25 mm) was obtained from Aldrich. All samples were treated by mechanically polishing with alumina and distilled water on a microcloth, followed by rinsing in distilled water and degreasing with acetone. Aluminum was not detected by XPS on the surface of the samples as a result of this polishing. The samples were not argon ion etched to avoid etching effects that we have previously reported.[14]

The polished samples were placed in the anaerobic cell and were subsequently characterized by XPS before the experiments were performed. Each of the experiments used 0.5 M sulfuric acid as the electrolyte. All solutions used for the experiments were made with triply distilled water. The solutions were deaerated with argon gas of 99.99% purity that was obtained from the Oxygen Service Co. All of the molybdenum metal samples were cathodically polarized at −0.5 V for 5 min in order to reduce any surface oxygen to the metal state and were then treated in the 0.5 M sulfuric acid at the following potentials, each for a period of 10 s: (a) −0.5, (b) 0.0, (c) 0.5, (d) 1.0, (e) 1.5, and (f) 2.0 V, all with respect to the saturated calomel electrode (SCE).

A second set of experiments was performed for the purpose of studying the time dependence of the oxide film formation. The sample treated at 2.0 V for 10 s described above was compared to a sample treated at 2.0 V for 30 s and a sample treated at 2.0 V for 2 min, using the same electrolyte and same polarization conditions as listed above, all with respect to SCE.

After the experiments were performed, the sulfuric acid was drained from the sample and the sample was rinsed five times with triply distilled water to remove any residual acid. The samples were then transferred into the XPS chamber for analysis. All samples were tested for oxidation at both bulk-sensitive (50°) and surface-sensitive (5°) takeoff angles. The S 2p spectrum for each sample was obtained and showed no detectable sulfur.

Data Analysis. The spectra were fitted using a nonlinear least-squares method with a Gaussian−Lorentzian peak shape[19−21] including the effect of X-ray satellites, with a nonlinear background included in the fitting process.[22,23] We have recently discussed[23] the effect of choosing different background removal methods in fitting oxidized molybdenum spectra and found that an iterative nonlinear background [22] gives the best agreement with the data. Use of the Tougaard background removal method[24] over the short energy ranges used in detailed spectral scans (15−25 eV) gives rise to what could be construed as metal oxide peaks that are, in fact, part of the background.[23] The Gaussian−Lorentzian mixing ratio was 0.5 for the metal oxide peaks and was 0.88 for the metal peaks. Exponential asymmetric tailing was added to the metal peaks in the molybdenum spectra to account for conduction band interaction effects. All the fitting parameters, such as peak position, peak width, and the separation between the main peak and the satellites were chosen according to previous data and curve-fitting results for standard compounds. The metal peaks were fitted so that they changed in the iterative process in such a way that their relative area was 1:1.5, but the $3d_{5/2}$ component had a full width at half-maximum (fwhm) of 0.8 times the fwhm of the $3d_{3/2}$ component. This difference in the peak widths was used in order to account for Coster−Kronig broadening.[25]

Band structure calculations were performed using a modified version of the program CRYSTAL (QCPE 577) and a substantially modified version of the program BNDPKG2 (part of the MOTECC90 suite of programs, copyright IBM). All calculations were performed on an IBM RISC/6000 computer. The density of states were adjusted by the Schofeld cross-section values,[26] with the Mo 5p level taken as having the same value as the Mo 5s level. This adjusted density of states was convoluted with a 2.3 eV fwhm 50% Gaussian−Lorentzian product function.[20,21] This function included the X-ray satellite peaks for the Mg X-radiation used.

Results and Discussion

Interpreting the Valence Band Spectra−Band Structure Calculations. Before discussing the results of the study, it is useful to evaluate the utility of valence band XPS for distinguishing between species in the molybdenum−oxygen system. We have already presented the valence band data for many compounds in this system in a previous paper,[14] so these spectra will not be presented here. In this earlier work[14] we reported the interpretation of these spectra by multiple-scattered-wave Xα calculations. In this paper we will evaluate the validity of this approach by discussing the use of band structure calculations to predict these spectra.

Figures 3−5 of our earlier paper[14] show the experimental and calculated valence band spectra for Mo, MoO_2, and MoO_3. In this work we will focus on the valence band region closest to the Fermi edge with a binding energy below 16 eV and will extend the calculations to include MoO and Mo_2O_5. In our earlier work we interpreted these valence band spectra using multiple-scattered wave Xα calculations on small ionic clusters. In this work we calculate the spectra using ab initio band structure calculations. In the case of the metal we have used an extended basis set calculation using the approach described by Callaway and co-workers.[27] This calculation is an all-electron self-consistent calculation based on the local-density approximation in density functional theory and employing the linear combination of Gaussian orbitals method. Our results were identical with those of Callaway and co-workers, and so they are not discussed here. However we extended this work by adjusting the density of states (Figure 1a) by the photoelectron cross sections to give a modified density of states which is shown in Figure 1b. Figure 1 only shows the density of states up to the Fermi level which has been slightly shifted from the

(18) Annual Book of ASTM Standards, vol. 03.05, *SIA, Surf. Interface Anal.* **1991**, *17*, 889.
(19) Ansell, R. O.; Dickinson, T.; Povey, A. F.; Sherwood, P. M. A. *J. Electroanal. Chem. Interfac. Electrochem.* **1979**, *98*, 79.
(20) Sherwood, P. M. A. *Practical Surface Analysis by Auger and Photoelectron Spectroscopy;* Briggs, D., Seah, M. P., Eds.; Wiley: London, 1983; Appendix 3.
(21) Sherwood, P. M. A. *Practical Surface Analysis by Auger and Photoelectron Spectroscopy*, 2nd ed.; Briggs, D., Seah, M. P., Eds.; Wiley: London, 1990, Appendix 3.
(22) Proctor, A.; Sherwood, P. M. A. *Anal. Chem.* **1982,** *54*, 13.
(23) Sherwood, P. M. A. *J. Vac. Sci. Technol.*, in press.
(24) Tougaard, S. *Surf. Sci.* **1989**, *216*, 343.
(25) Måartenson, N.; Nyholm, R. *Phys. Rev. B* **1982,** *25*, 4452.
(26) Scofeld, J. H. *J. Electron Spectrosc. Relat. Phenom.* **1976**, *8*, 129.
(27) Jani, A. R.; Tripathi, G. S.; Brener, N. E.; Callaway, J. *Phys. Rev. B* **1989**, *40*, 1593.

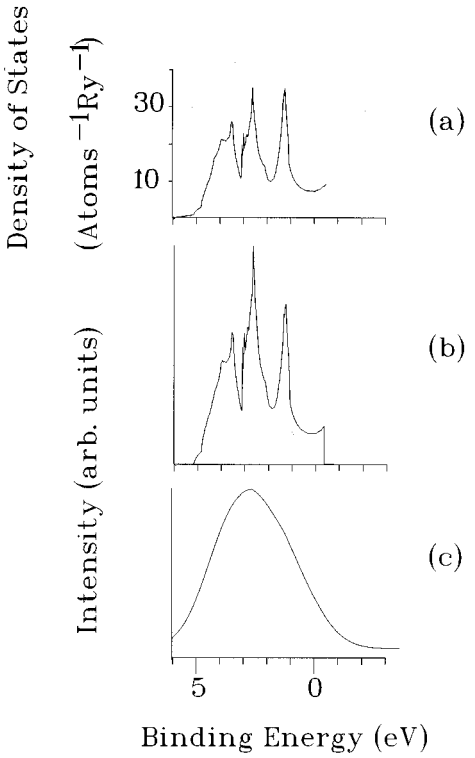

Figure 1. Density of states and predicted valence band spectrum for b.c.c. molybdenum metal obtained by an accurate band structure calculation. The density of states is shown in (a), the density of states adjusted by the photoelectron cross sections is shown in (b), and (c) shows the data in (b) convoluted with a 2.3 eV Gaussian−Lorentzian product function.

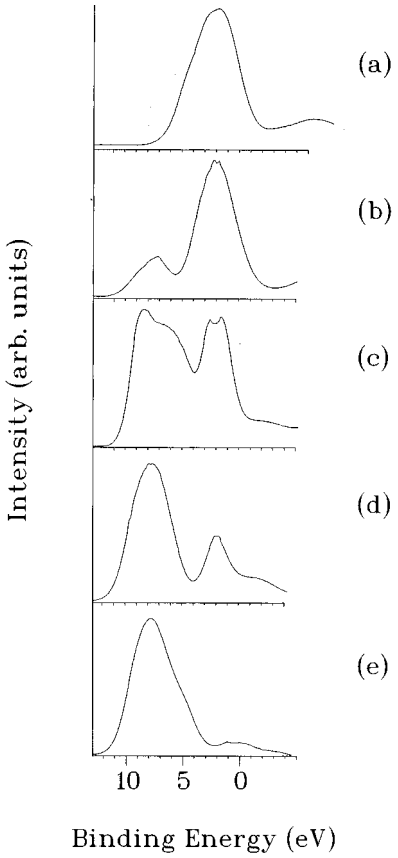

Figure 2. Calculated valence band spectra from band structure calculations. (a) Molybdenum metal, (b) MoO, (c) MoO_2, (d) Mo_2O_5, (e) MoO_3.

calculated value (−0.3576 eV). Figure 1c shows the result of convoluting this adjusted density of states with the Gaussian−Lorentzian product function described above. This calculation gives results almost identical with those of other very accurate band structure calculations (e.g., refs 28 and 29 and the references therein). In going from the simple body-centered cubic structure of the metal with its monatomic unit cell to the lower symmetry geometries of the oxides, we had to increase the level of approximation including a simplification of the basis set to a simple STO-3G basis set. MoO was taken as a cubic structure ($Fm3m$) with $a = 5.019$Å[30] with one molybdenum and one oxygen atom in the unit cell. MoO_2 was taken as a monoclinic ($P2_1/c$) with a 12 atom unit cell containing 4 Mo and 8 O atoms.[31] Mo_2O_5 is known as a violet compound obtained by heating a mixture of Mo and MoO_3 in stoichiometric quantities at 750 °C. However, its crystal structure has not been reported, so we have taken an imaginary crystal structure based upon the orthorhombic ($Pmmn$) V_2O_5 structure with Mo−O distances of 1.72085(×1), 1.93199 (×1), and 2.0373 (×2) Å. The unit cell contained 14 atoms, 4 Mo and 10 O atoms. MoO_3 was taken as an orthorhombic structure ($Pbnm$) with a 16 atom unit cell with 4 Mo and 12 O atoms. Figure 2 shows the calculated spectra obtained in a manner similar to that of Figure 1c. The separations between the energy levels were contracted by a factor of 1.3 for all the results shown in Figure 2. This was done following a comparison between a simple STO-3G basis set calculation for the metal with the extended basis set calculation shown in Figure 1. The 1.3 contraction gives a calculated spectrum and a density of states whose density of states maxima compare well for the metal in Figures 1 and 2. We thus conclude that the 1.3 contraction represents a reasonable adjustment to apply to the less accurate band structure peak separations.

The calculated spectra indicate that two peaks should be seen in the near Fermi edge region for MoO, MoO_2, and Mo_2O_5, and a single peak in the case of MoO_3. In the case of MoO the low binding energy peak would be expected to be predominant, and in the case of Mo_2O_5 the high binding energy peak would be expected to be predominant. These results agree with those of the earlier cluster calculations[14] for MoO_2 and Mo_2O_5. A more detailed examination of the predicted spectrum for MoO_2 shows (Figure 3) that the low binding energy peak should be narrower than the high binding energy peak, in agreement with the experimental data. In the cluster calculations both peaks[14] were predicted to be of approximately equal width. We believe that the reason for this difference can be understood by considering the dispersion relations for the occupied levels. In the case of MoO_2 it is clear that the width of the group of bands making up the high binding energy feature is considerably broader than those making up the low binding energy feature. Another aspect of the dispersion relations is that it is clear that the bands show considerable dispersion in the case of the metal but that

(28) Bacalis, N. C.; Blathras, K.; Thomaides, P. *Phys. Rev. B* **1985**, *32*, 4849.
(29) Koelling, D. D.; Mueller, F. M.; Arko,A. J.; Ketterson, J. B. *Phys. Rev. B* **1974**, *10*, 4889.
(30) Aubry, J. *Nouv. Traité Chim. Miner.* **1959**, *14*, 635.
(31) Brandt, B. G.; Skapski, A. C. *Acta. Chem. Scand.* **1967**, *21*, 661.

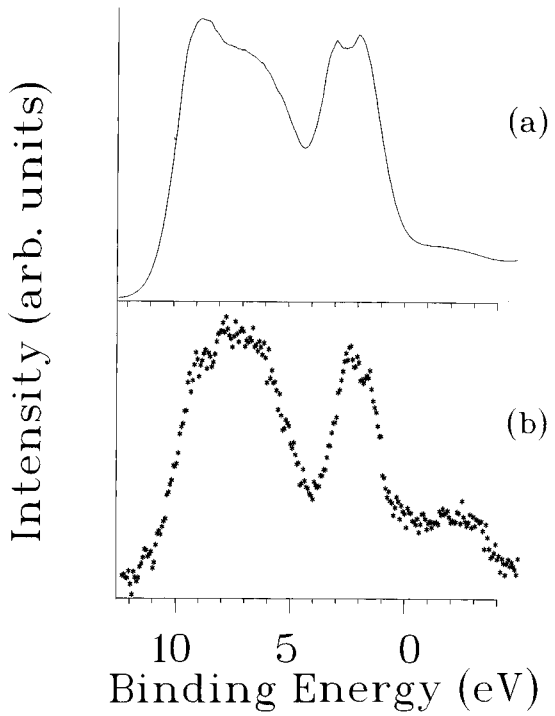

Figure 3. Calculated (a) and experimental (b) valence band spectra for MoO_2.

Table 1. Molybdenum/Oxygen Area Ratios

	based upon Mo 3d/O 1s area ratio		based upon Mo 4p/O 2s area ratio	
sample treatment	50° takeoff angle	5° takeoff angle	50° takeoff angle	5° takeoff angle
as received	0.30	0.20	0.33	0.30
polished	0.43	0.13	0.75	0.53
−0.5 V	0.64	0.42	0.83	0.38
0.0 V	0.42	0.28	0.96	0.62
0.5 V	0.47	0.42	0.61	0.58
1.0 V	0.41	0.35	0.53	0.44
1.5 V	0.38	0.34	0.52	0.45
2.0 V, 10 s	0.35	0.31	0.49	0.40
2.0 V, 30 s	0.33	0.33	0.54	0.50
2.0 V, 2 min	0.41	0.42	0.51	0.49

the bands become relatively flat in the case of the oxides. This observation supports the use of cluster models for the oxides.

Surface Analysis. C 1s, O 1s, Mo 3d, S 2p, overall, and valence band spectra were recorded for each sample. Only the O 1s, Mo 3d, and valence band spectra will be discussed in detail. Table 1 gives a rough approximation of the relative amounts of molybdenum with respect to the amount of oxygen on the sample surface. All of the atomic ratios assume that the data come from a homogeneous mixed Mo/O region, which is a very crude model. The atomic ratios were adjusted for differences in photoelectron cross-section and analyzer transmission function and use a nonlinear background[22] rather than the linear sloping background used in our earlier work.[14] Two different regions are shown for the area ratios. The Mo 3d/O 1s ratio shows a ratio for regions that are more surface sensitive and the Mo 4p/O 2s ratio shows a region that is less surface sensitive. The Mo 4p/O 2s ratio was obtained by subtracting the $K\alpha_{3,4}$ X-ray satellite intensity from the spectrum and removing a nonlinear background[22] from the Mo 4p and O 2s regions. In fact the average inelastic mean free path (averaging over the metal, MoO_2, and MoO_3, using the Seah and Dench equations[35]) is in the ratio 1:1.2:1.3 for the O1s, Mo3d, and Mo4p/O2s regions. In addition it should be pointed out that the calculated inelastic mean free paths follow the order $MoO_3 > MoO_2 > Mo$ with an approximate ratio of 1:0.9:0.6, meaning that the experiments will be less sensitive to metal than oxide as one goes into the surface. The Mo 3d/O 1s ratio was corrected for differences in inelastic mean free path for the Mo 3d and O 1s regions. As would be expected, the atomic ratio is always lower for the surface-sensitive angle (5°) than for the bulk-sensitive angle (50°), and the atomic ratios are greater for the Mo 4p/O 2s ratio than the Mo 3d/O 1s ratio. This pattern is indicative of a greater amount of oxygen-containing species on the surface of the metal than in the bulk region. As will be discussed below, these oxygen-containing species may be water, oxides, or hydroxides of molybdenum. Cases where there is a large difference between the Mo 3d/O 1s and Mo 4p/O 2s ratios are seen only for the polished, −0.5 and 0.0 V samples, cases where the predominant species is metal, and the oxide present is likely to be in a patchy and inhomogeneous form. One notes that the as-received metal, which will be seen below to consist of a surface MoO_3 layer, corresponds to the expected 0.33 ratio at the bulk-sensitive take-off angle. The 2.0 V, 30 s, and 2 min samples show similar atomic ratios for both bulk and surface-sensitive angles, indicating that the surface probed has a uniform composition, rather than a layer structure, in these cases. This will be discussed further below.

The O 1s spectra were fitted to two or three peaks. The Mo 3d spectra were fitted to one spin−orbit split pair of metal peaks and one or two spin−orbit split pairs of metal oxide peaks. These fitted spectra are shown in Figure 4. It should be made clear that, as in any curve-fitting process, the fit is not a unique fit, but rather one possible fit to the data. The uncertainty shown in the tables represents the 95% confidence limits obtained from the fit shown and does not imply that the shown fit has any uniqueness. In fitting the data, we made a number of assumptions that were applied to all the fits:

(a) In the O 1s spectra the fwhm of each of the two- or three-component peaks was fixed to be the same for each spectrum fitted and was fixed so that it took the same value for the surface-sensitive angle (5°) and the bulk-sensitive angle (50°) for spectra collected from the same sample.

(b) In the Mo 3d spectra the fwhm of the metal peak at 227.6 eV was fixed to be the same for the whole series of spectra fitted. The fwhm of the oxide was fixed so that it took the same value for all oxidized species and took the same value for the surface-sensitive angle (5°) and the bulk-sensitive angle (50°) for spectra collected from the same sample.

First the spectral features will be discussed, followed by a discussion of how the spectra of samples treated at 2.0 V depended upon polarization time.

O 1s Region. This region is valuable for distinguishing the differences in oxidation product for the various

(32) Kihlborg, L. *Ark. Kem.* **1963**, *21*, 357.
(33) Dickinson, T.; Povey, A. F.; Sherwood, P. M. A. *J. Chem. Soc., Farada Trans. 1* **1976**, *76*, 686.
(34) Carlson, T. A.; McGuire, G. E. *J. Electron Spectrosc. Relat. Phenom.* **1972/3**, *1*, 161.
(35) Seah, M. P.; Dench, W. A. *Surf. Interface Anal.* **1979**, *1*, 2.

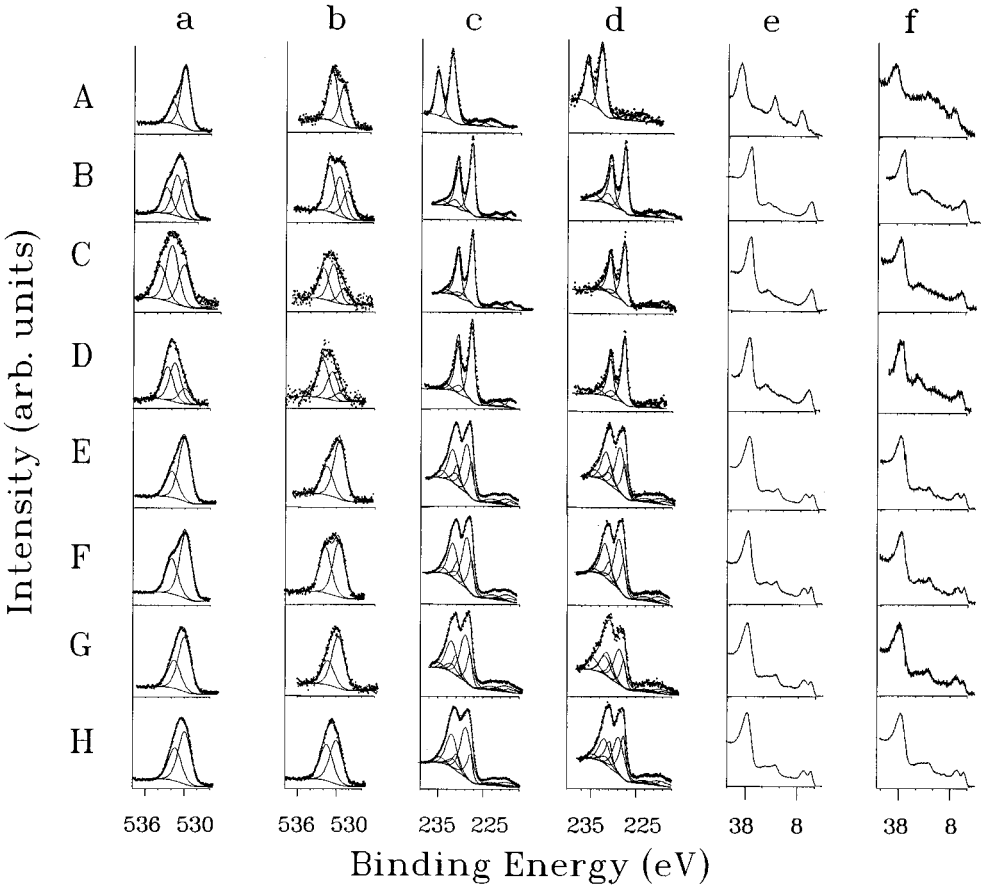

Figure 4. Molybdenum metal spectra for various potential treatments of molybdenum metal samples. (A) Molybdenum metal as received. (B) Molybdenum metal polished. (C) Molybdenum metal polarized to −0.5 V. (D) Molybdenum metal treated at 0.0 V for 10 s. (E) Molybdenum metal treated at 0.5 V for 10 s. (F) Molybdenum metal treated at 1.0 V for 10 s. (G) Molybdenum metal treated at 1.5 V for 10 s. (H) Molybdenum metal treated at 2.0 V for 10 s. (a) 50° O 1s core spectrum. (b) 5° O 1s core spectrum. (c) 50° Mo 3d core spectrum. (d) 5° Mo 3d core spectrum. (e) 50° valence band spectrum. (f) 5° valence band spectrum.

sample treatments. Details of the curve-fitting process are given in Table 2. The data illustrate clearly the reason for the lowering Mo/O ratio for the surface-sensitive angle. The oxygen-containing species adsorbed on the molybdenum surface in the O 1s region are H_2O, OH^-, and O^{2-}, at binding energies of 533.3, 532.2, and 530.1 eV, respectively. In a previous study, we found that molybdenum metal had a high affinity for water after exposure to pure, deaerated water.[14] In this study we see no clear evidence for water under conditions where significant amounts of surface oxides are formed (Figure 4E−H). However, some water is seen, as expected, on the polished metal where the surface is not significantly oxidized (Figure 4B−D). The presence of three peaks in these cases is not essential for fitting the data, and Table 2 shows under (A) the result of fitting the data to two- rather than three-peaks (shown in (B)). Differences in the χ^2 values for a two or three peak fit are not large enough to conclude that one or the other is more reasonable, but Table 2 indicates that the two-peak fit requires component peaks with a much larger fwhm than the three-peak fits. We feel that the use of three peaks, which indicates that some surface water is adsorbed on the metal, is not inconsistent with the data and thus can be presented as one reasonable interpretation of the O 1s spectra for samples with a large surface metal content. The bulk-sensitive as-received sample shown in Figure 4A(a) gives spectra indicative of mainly oxide oxygen, with some hydroxide present. The surface-sensitive spectrum (Figure 4A(b)) indicates that the hydroxide peak is more intense than the oxide peak, indicating that the outermost layer of oxygen is adsorbed as hydroxide oxygen, and beneath it a layer of oxide oxygen is present. As can be seen from the spectra in Figure 4B, the polishing process removes most of the oxide from the surface, but some oxide and hydroxide oxygen and water is still present. The spectra at a surface-sensitive angle shows the relative amount of water to increase, which indicates that the water lies at the outer surface of the sample.

Cathodic polarization of the polished metal causes the relative oxide intensity to decrease from that found in the polished sample, but a small amount of oxide and hydroxide is left on the surface, as can be seen in Figure 4C. As stated above, the presence of H_2O on the surface is consistent with the previous results, as the amount of oxide on the sample surface is low with respect to that of the samples treated at higher potentials. The relative amount of hydroxide present on the surface of the sample decreases slightly at surface-sensitive angles, but the proportion of water increases. The amount of oxide present on the sample surface also decreases in a greater amount than does the hydroxide, indicating that the oxide is closer to the metal than is the water or hydroxide, as would be expected. Application of 0.0 V shows a decrease in the relative amount of oxide from the bulk to surface-sensitive spectrum, as can be seen in Figure 4D. The amount of hydroxide present decreases and the amount of water increases for this sample, indicating that a similar water adsorption

Table 2. Curve-Fitting Results for the O 1s Core XPS Region[a]

	O^{2-}				OH^-				H_2O			
	peak		%		peak		%		peak		%	
sample treatment	50°	5°	50°	5°	50°	5°	50°	5°	50°	5°	50°	5°
as received	530.1	530.1	74.1	43.7	531.8	531.8	25.9	56.3				
uncertainty[b]			(1.0)	(2.3)			(1.2)	(2.2)				
fwhm	1.8	1.8			1.8	1.8						
polished(A)	530.1	530.1	66.6	51.7	532.1	532.1	33.4	48.3				
uncertainty			(1.2)	(2.0)			(1.7)	(2.0)				
fwhm	2.4	2.4			2.4	2.4						
polished(B)	530.1	530.1	36.7	24.3	531.3	531.3	38.8	34.4	532.9	532.9	24.5	41.3
uncertainty			(2.0)	(1.4)			(2.2)	(1.2)			(2.2)	(1.3)
fwhm	1.9	1.9			1.9	1.9			1.9	1.9		
−0.5 V(A)	530.1	530.1	50.7	29.5	531.9	531.9	49.3	70.5				
uncertainty			(5.1)	(10.6)			(5.1)	(8.5)				
fwhm	1.9	1.9				1.9	1.9		1.9	1.9		
−0.5V(B)	530.1	530.1	31.5	18.5	531.7	531.7	43.3	44.7	533.2	533.2	25.2	36.9
uncertainty			(2.4)	(4.5)			(2.5)	(4.2)			(2.5)	(5.7)
fwhm	2.1	2.1			2.1	2.1			2.1	2.1		
0.0 V(A)	530.1	530.1	27.4	36.7	531.7	531.7	72.6	63.3				
uncertainty			(5.0)	(8.3)			(3.4)	(7.2)				
fwhm	3.0	3.0			3.0	3.0						
0.0 V(B)	530.1	530.1	17.7	11.3	531.6	531.5	44.6	37.7	532.7	532.7	37.7	51.0
uncertainty			(4.5)	(5.3)			(8.5)	(6.2)			(8.7)	(6.4)
fwhm	2.5	2.5			2.5	2.5						
0.5 V	530.1	530.1	70.7	66.9	532.1	532.1	29.4	33.1				
uncertainty			(1.1)	(1.6)			(1.4)	(1.8)				
fwhm	2.2	2.2			2.2	2.2						
1.0 V	530.1	530.1	64.7	54.7	532.2	532.2	35.3	45.3				
uncertainty			(1.0)	(1.5)			(1.1)	(1.5)				
fwhm	2.2	2.2			2.2	2.2						
1.5 V	530.1	530.1	66.3	68.1	531.7	531.7	33.8	31.9				
uncertainty			(2.0)	(3.1)			(2.8)	(3.6)				
fwhm	2.3	2.3			2.3	2.3						
2.0 V	530.1	530.1	61.4	54.6	531.6	531.6	38.6	45.4				
uncertainty			(2.1)	(2.7)			(3.0)	(2.8)				
fwhm	2.3	2.3			2.3	2.3						

[a] % = % area of the O 1s core XPS region. Peak = peak center. [b] Values represent 95% confidence limits for the peak area. (A) refers to a fit with two peaks, (B) to a fit with three peaks. Where (A) and (B) are not indicated, the fit is to two peaks.

process occurs as for the −0.5 V sample. As the active region of molybdenum is entered, the 0.5 V sample shows that the level of surface oxidation increases significantly over the 0.0 V sample, with a growth in oxide intensity in both the surface and bulk-sensitive spectra (Figure 4E). The relative amount of hydroxide decreases with respect to the 0.0 V sample, with a greater presence of hydroxide in the surface-sensitive sample, indicating that the hydroxide is closer to the surface. The 1.0 V spectra reveal a relative increase in hydroxide intensity, which is especially noticeable in the surface-sensitive spectrum as the higher binding-energy component intensity (OH^-) increases with respect to the lower binding-energy component (O^{2-}). The 1.5 V sample shows a significant increase in the oxide intensity with respect to the hydroxide intensity at both angles. The 2.0 V sample shows a large oxide peak with an increase in the hydroxide peak from the 1.5 V sample.

Mo 3d Region. Molybdenum has a relatively large number of oxidation states whose characteristic Mo 3d binding energies are indicated in Table 3. The features of the Mo 3d region may include molybdenum oxide peaks in the higher binding energy region of the spectrum, molybdenum metal peaks in the lower binding energy region of the spectrum, and the $K\alpha_{3,4}$ satellites at the lowest binding energy end of the Mo 3d spectrum. Fitting of the complex Mo 3d spectra can never lead to a unique solution. In this work we have used the fitting constraints discussed above. Three qualitative types of Mo 3d spectra can be noted:

Table 3. Binding Energies for the Various Molybdenum Oxidation States

oxidation state	Mo $3d_{3/2}$, eV	Mo $3d_{5/2}$, eV
Mo(0)	230.8	227.6
Mo(III)	231.5	228.3
Mo(IV)	232.3	229.3
Mo(V)	234.0	230.8
Mo(VI)	235.4	232.2

(a) Spectra whose appearance is predominantly that of the metal, with a small amount of oxide present (Figure 4B−D). These spectra can be fitted to a metal spin−orbit split doublet and an oxide spin−orbit split doublet.

(b) Spectra where substantial amounts of oxidation is present characterized by two approximately equal-intensity Mo 3d peaks, separated by a valley, that appear substantially broader than the principally metal spectra of type (a). These spectra can be fitted to a metal spin−orbit doublet, and two oxide spin−orbit split doublets with the lower binding energy oxide doublets being the predominant oxide constituent. These are found in Figures 4E−H.

(c) Spectra that show three overlapped peaks with little or no valley between the peaks and a central peak of higher intensity than the approximately equal intensity peaks to its right and left. These spectra can be fitted to a metal spin−orbit doublet, and two oxide spin−orbit split doublets with the higher binding energy oxide doublets being the predominant oxide constituent. In addition there is the single oxide doublet found for the as-received sample.

Table 4. Curve-Fitting Results for the Mo 3d Core XPS Region

	Mo metal				MoO_2				MoO_3			
	peak[a]		%		peak[a]		%		peak[a]		%	
sample treatment	50°	5°	50°	5°	50°	5°	50°	5°	50°	5°	50°	5°
as received			0.0	0.0			0.0	0.0	232.2	232.2	100.0	100.0
uncertainty[b]											(1.5)	(2.3)
fwhm									1.9	1.9		
polished	227.6	227.6	85.3	79.5			0.0	0.0	231.5	231.5	14.7	20.5
uncertainty			(1.4)	(1.1)							(1.2)	(1.0)
fwhm	1.1	1.1							2.6	2.6		
−0.5 V	227.6	227.6	88.4	86.8			0.0	0.0	230.4	230.4	11.6	13.2
uncertainty			(1.0)	(2.7)							(0.9)	(1.0)
fwhm	1.1	1.1							2.6	2.6		
0.0 V	227.6	227.6	85.5	83.9			0.0	0.0	230.5	230.5	14.5	16.1
uncertainty			(2.4)	(2.9)							(2.2)	(2.7)
fwhm	1.1	1.1							2.5	2.5		
0.5 V	227.6	227.6	27.2	27.1	228.7	228.7	59.6	58.6	231.1	231.1	13.2	14.3
uncertainty			(1.7)	(3.0)			(1.4)	(2.5)			(0.8)	(1.4)
fwhm	1.1	1.1			2.6	2.6			2.6	2.6		
1.0 V	227.6	227.6	26.3	26.6	228.7	228.7	63.5	66.4	231.0	231.0	10.2	7.0
uncertainty			(0.7)	(2.5)			(0.9)	(2.1)			(0.7)	(1.1)
fwhm	1.1	1.1			2.6	2.6			2.6	2.6		
1.5 V	227.6	227.6	28.2	21.6	228.7	228.5	63.6	51.1	231.8	231.8	11.4	27.3
uncertainty			(1.6)	(2.0)			(1.6)	(2.6)			(0.9)	(1.5)
fwhm	1.1	1.1			2.9	2.9			2.9	2.9		
2.0 V	227.6	227.6	22.7	38.3	228.8	228.8	56.6	51.3	231.4	231.4	11.9	10.4
uncertainty			(1.4)	(1.3)			(1.3)	(1.6)			(0.8)	(0.9)
fwhm	1.1	1.1			2.9	2.9			2.9	2.9		

[a] Values given are for the Mo $3d_{5/2}$ component. % = % area of the Mo 3d core XPS region. Peak = peak center. [b] Values represent 95% confidence limits for the peak area.

Figure 4 shows Mo 3d spectra of types (a) and (b). Mo 3d spectra of type (c) are found for 2.0 V samples polarized for longer time periods, and these spectra will be discussed later.

Details of the curve-fitting process are given in Table 4. The as-received molybdenum metal sample gives a Mo 3d region (Figure 4A(c,d)) that indicates that the surface consists entirely of MoO_3, with the Mo $3d_{5/2}$ component occurring at 232.2 eV and the Mo $3d_{3/2}$ component occurring at 235.4 eV. The polished metal sample (Figure 4 (c,d)) shows the metal peaks, indicated by the two narrow peaks at 227.6 eV for the Mo $3d_{5/2}$ component and at 230.1 eV for the Mo $3d_{3/2}$ component, as well as a small amount of MoO_3 that remains on the metal surface, which occurs at 231.5 eV for the Mo $3d_{5/2}$ component and at 234.7 eV for the Mo $3d_{3/2}$ component. The residual MoO_3 is probably present in patches as there is no significant increase in its relative intensity at surface-sensitive angles. The polished metal samples polarized to −0.5 and 0.0 V (Figure 4C(c,d) and Figure 4D(c,d), respectively) give a spectrum similar to that of the polished metal, as this reducing region would not be expected to form any oxide. The metal sample treated to 0.5 V for 10 s reveals substantial oxidation with respect to the polished metal sample leading to the type (b) spectrum discussed above. The oxidation is indicated by the decrease of the valley between the metal spin−orbit splitting components, as well as the broadening of the $K\alpha_{3,4}$ satellite features below 225 eV. The fitted spectrum indicates lower binding energy components are characteristic of the metal peaks, Mo(0), and higher binding energy components are characteristic of oxidized molybdenum. Two oxidized species are found. One has a binding energy consistent with Mo(IV) and the other a binding energy in the Mo(VI) region. The spectrum of the sample treated at 1.0, 1.5, and 2.0 V for 10 s also shows substantial oxidation and a similar spectrum and relative amounts of metal and different types of oxide. There is little difference in the relative amounts of the various components in the spectrum at the bulk and surface-sensitive angles, indicating that the surface film probed is fairly homogeneous in composition with depth. This point will be discussed further below. In the case of the sample treated at 2.0 V for 10 s the metal component seems to increase in relative intensity in the surface-sensitive spectrum. The behavior at 2.0 V will be discussed further below. The background choice played an important role in determining both the number of oxides and the types of oxide present in the spectra. We have already discussed the importance and the effects of background choice in fitting these spectra.[23]

Table 5. Comparison between Valence Band Height Ratio and Core Metal Percentage

sample treatment	height ratio (valence band)		core metal percentage (Mo 3d)	
	50°	5°	50°	5°
0.5 V	0.77	0.72	27.2	27.1
1.0 V	0.69	0.75	26.3	26.6
1.5 V	0.78	0.98	28.2	21.6
2.0 V (10 s)	0.74	0.75	22.7	38.3
2.0 V (30 s)	1.05	1.14	13.1	18.6
2.0 V (2 min)	1.11	1.12	21.7	18.8

The binding energy of the species attributed to MoO_3 varies from 532.2 eV for the as-received sample which we know represents a surface of MoO_3 to 230.5 eV in some of electrochemically treated samples in Tables 4 and 6. Table 3 assigns the value of 230.8 eV to Mo_2O_5. However, this binding energy is a suggestion that we and others have made for the binding energy of Mo_2O_5. Mo_2O_5 is not a well-defined compound so that we do not have data in the oxide itself. We will discuss other aspects of an expected Mo_2O_5 spectrum below, but clearly it is possible that binding energies in the vicinity of 230.8 eV may correspond to Mo_2O_5.

Valence Band Region. The major features in the valence band region for molybdenum are the Mo 4p peak

Table 6. Curve-Fitting Parameters for the 2.0 V Time-Dependent Study

		O^{2-}		OH^-		Mo		MoO_2		MoO_3	
sample treatment		peak	%	peak	%	peak[a]	%	peak[a]	%	peak[a]	%
2.0 V,10 s	50°	530.1	61.4	531.6	38.6	227.6	22.7	228.8	56.6	231.4	11.9
	uncertainty[b]		(2.1)		(3.0)		(1.4)		(1.3)		(0.8)
	fwhm		2.3		1.1		2.9		2.9		
	5°	530.1	54.6	531.6	45.4	227.6	38.3	228.7	51.3	231.2	10.4
	uncertainty[b]		(2.7)		(2.8)		(1.3)		(1.6)		(0.9)
	fwhm	2.3		2.3		1.1		2.9		2.9	
2.0 V,30 s	50°	530.1	74.7	532.0	25.3	227.6	13.1	228.4	37.1	230.9	49.8
	uncertainty[b]		(1.0)		(1.2)		(1.5)		(1.9)		(1.4)
	fwhm	2.0		2.0		1.1		2.9		2.9	
	5°	530.1	72.1	532.0	27.9	227.6	18.6	228.4	37.1	230.9	44.3
	uncertainty[b]		(2.0)		(2.0)		(1.7)		2.8)		(2.0)
	fwhm	2.0		2.0		1.1		2.9		2.9	
2.0 V,2 min	50°	530.1	78.8	532.0	21.2	227.6	21.7	228.4	23.5	230.7[c]	54.8
	uncertainty[b]		(1.04)		(1.3)		(1.2)		(1.6)		(1.2)
	fwhm	2.0		2.0		1.1		2.9		2.9	
	5°	530.1	76.2	532.0	23.8	227.6	18.8	228.4	24.6	230.7[c]	56.6
	uncertainty[b]		(1.3)		(1.3)		(1.2)		(1.6)		(1.0)
	fwhm	2.0		2.0		1.1		2.9		2.9	

[a] Values given are for the Mo $3d_{5/2}$ component. % = % area of the Mo 3d core XPS region. Peak = peak center. [b] Values represent uncertainty in the peak area. [c] May be Mo_2O_5; see text for discussion.

near 40 eV, the O 2s peak around 23 eV, and the outer valence band region centered near 5 eV. The features near 28 eV are the $K\alpha_{3,4}$ satellites from the Mo 4p peak. The as-received metal shows a significant O 2s peak at 23 eV, indicating the presence of a surface layer of MoO_3. A single peak is also present in the outer valence band region that is characteristic of MoO_3, as predicted in the spectrum shown in Figure 2.

The polished metal sample has features that include only the Mo 4p peak, the $K\alpha_{3,4}$ satellites, and a single peak in the outer valence band region that is characteristic of the metal and agrees with the predicted spectrum shown in Figure 2. This single peak is shifted to about 5 eV lower binding energy from the single peak for MoO_2 as expected from the calculations.

The samples polarized to −0.5 and 0.0 V show spectra that are very similar to that of the polished metal sample, with no detectable increase in the O 2p intensity or shift in the outer valence band region peak from the polished metal sample position of 2 eV.

An expanded valence band region, after the removal of a nonlinear background, near the Fermi edge is shown for the electrochemically oxidized samples in Figure 5. This figure allows comparisons with Figure 2 to be easily made. Two peaks are seen in all these spectra, the metal spectrum having a single peak at the position of the low binding energy peak in Figure 5. The valence band spectrum of the metal that was treated at potentials greater than 0 V show an increase in the intensity of the O2s feature at 23 eV, and the appearance of two peaks in the outer valence band region, rather than the single peak seen for the metal. These two peaks could arise from a combination of the spectra of MoO_2, Mo_2O_5, and MoO_3 with that of the metal. It should be noted that the metal component of the Mo(0) spectrum and the lower binding energy peak of the oxides (other than MoO_3 where this peak is absent) occur in about the same position and their intensities are additive. However, it should also be noted that the metal peak is broader than the lower binding energy oxide features. It seems unlikely that MoO is present, because Figure 2 shows that this would have only a low-intensity high binding energy component, and a MoO/Mo mixture could not correspond to the observed spectra

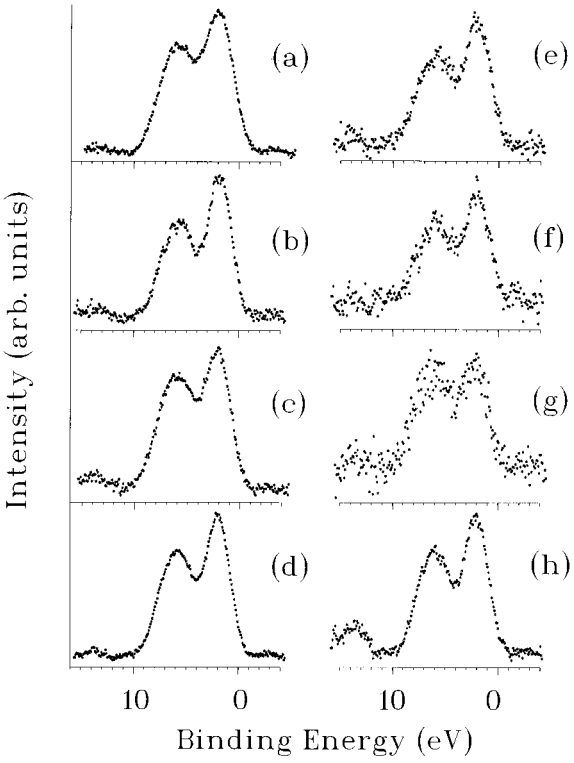

Figure 5. Near Fermi-edge valence band spectra for electrochemically oxidized molybdenum metal for 10 s at various voltages. (a) and (e) molybdenum polarized to 0.5 V at 50° and 5°. (b) and (f) molybdenum metal polarized to 1.0 V at 50° and 5°. (c) and (g) molybdenum metal polarized to 1.5 V at 50° and 5°. (d) and (h) molybdenum metal polarized to 2.0 V at 50° and 5°.

as such a mixture would have a high binding energy component of lower intensity than that shown in Figure 2b. It seems unlikely that any of the spectra correspond to that of MoO_2 alone for comparison with Figure 3 would suggest that the lower binding energy peak of this oxide should be broader than the high binding energy peak (see the discussion above). Thus the spectra in Figure 5 (where the two peaks are of comparable width) almost certainly contain a mixture of the oxides with metal, in agreement with the analysis of the Mo 3d region. Comparison between the valence

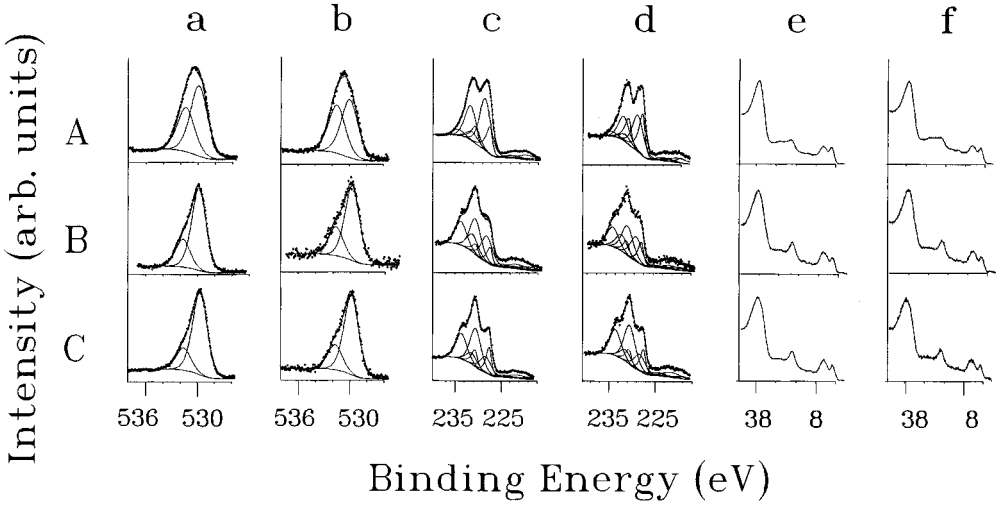

Figure 6. Molybdenum metal spectra for the time-dependent study. (A) Molybdenum metal sample treated at 20 V for 10 s. (B) Molybdenum metal sample treated at 2.0 V for 30 s. (C) Molybdenum metal sample treated at 2.0 V for 2 min. (a) 50° O 1s core spectrum. (b) 5° O 1s core spectrum. (c) 50° Mo 3d core spectrum. (d) 5° Mo 3d core spectrum. (e) 50° valence band spectrum. (f) 5° valence band spectrum.

band data and the fitting of the Mo 3d region must be qualified by the fact that the valence band region probes more deeply into the bulk than the Mo 3d region due to the higher kinetic energy of the valence band photoelectrons.

While a simple curve fitting is not appropriate because of the multiple peak nature of the oxidized molybdenum species, a crude qualitative measure can be obtained by comparing the ratio of the height of the high binding energy peak divided by the height of the low binding energy peak. This ratio is shown in Table 5, and the ratio is compared with the percentage metal character obtained from fitting the Mo 3d core region. In general, the ratio falls when the percentage of metal increases, as would be expected if a significant amount of the lower binding energy peak is due to metal.

The spectra in Figure 5 can reasonably be considered to be a mixture of MoO_2 and Mo. Also it is not unreasonable that Mo_2O_5 is present, though not in very large quantities because this would lead to a reduction in the intensity of the low binding energy peak with respect to the high binding energy peak. It is not possible to determine how much MoO_3 is present, but because this oxide contains only the high binding energy peak, any substantial amount of this oxide can be excluded. This is consistent with the type (b) spectrum discussed for the Mo 3d region above. When one combines the information obtained in the valence band region with that in the core region, it is clear that the curve fitting in the Mo 3d core region is consistent with the above interpretation of the valence band region, though differences in these two regions would be expected because of the greater depth probed by the valence band region. This latter point would lead one to expect a larger proportion of metal in the valence band region, which is not consistent with the results presented in Figure 5. The height ratio on going from a bulk to surface sensitive angle follows the trend in the Mo 3d region (Tables 4 and 5).

Time-Dependent Studies. We have examined the effect of changing the time of polarization on the electrochemical oxidation of molybdenum at 2.0 V. Figure 6 summarizes the results of this study, with the curve fitting of the core regions given in Table 6. Figure

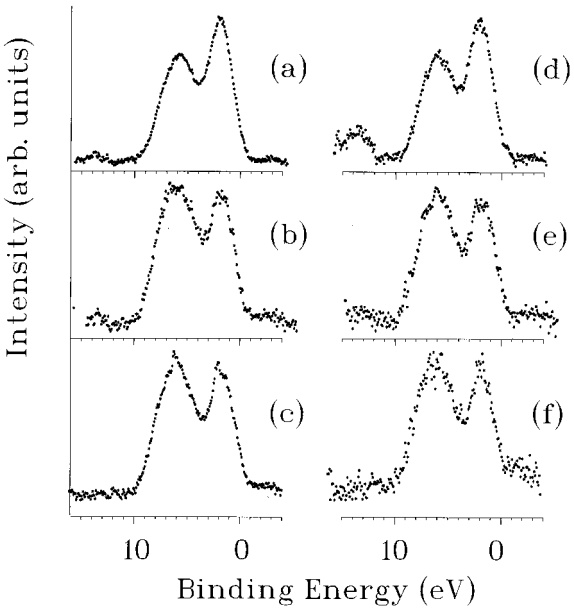

Figure 7. Near Fermi-edge valence band spectra for electrochemically oxidized molybdenum metal for various times at 2.0 V s voltages. (a) and (d) 10 s polarization at 50° and 5°. (b) and (f) 30 s polarization at 50° and 5°. (c) and (g) 2 min polarization at 50° and 5°.

7 shows the changes in the outer valence band region, with the changes in height ratio indicated in Table 5. The most important aspect of these studies is that the differences seen at 2.0 V from those of other potentials arises from significant changes in the mechanical stability of the oxide film. We can observe oxide falling off the oxidized metal surface in the case of oxide films formed after polarization to 2.0 V, the mechanical stability of this film appearing to become worse as the polarization time increases. Attempts to polarize the electrode at 2.0 V for longer than 2 min led to substantial loss of the oxide film, and thus we did not attempt longer polarization times than 2 min. The films that we examine by XPS in these 2.0 V polarization studies have suffered some loss of material by film instability, so the data reported represent a combination of the result of electrochemical oxidation and the mechanical loss of material from the structurally unstable films. The

spectral changes, however, do indicate a change from the type (b) Mo3d spectrum to the type (c) Mo3d spectrum corresponding to an increase in the relative intensity of higher binding energy and high oxidation state oxide film as the polarization time is increased. Such a change is consistent with the increase in oxidation represented by increasing polarization time.

The molybdenum sample that was treated for 10 s at 2.0 V shows a type (b) Mo3d spectrum. However, a relative *increase* in metal intensity at surface sensitive angle would be consistent with the mechanical loss of part of the film leading to some exposed underlying metal. Longer periods of polarization time lead to a type (c) Mo3d spectrum where the principal difference is the substantial increase in the amount of higher oxidation state and binding energy Mo species which increases from about 12% at 10 s to about 50% at 30 s and about 55% at 2 min. There is little change in the relative amounts of the different species with takeoff angle after 30 s and 2 min polarization. The O 1s region is similar at different takeoff angles for 30 s and 2 min polarization, but there is a decrease in O^{2-} intensity with respect to OH^- intensity in the O 1s region for the sample polarized for 10 s.

The valence-band region shows the presence of a single O 2s peak at 23 eV in the 30 s and 2 min polarized spectra. The O 2s region has a high O 2s character (as there is little mixing with Mo character in this region), and its behavior is similar to the O 1s region. The O 1s region shows a major increase in the relative amount of oxide component, which becomes the predominant component in the more bulk-sensitive valence band O 2s region. Figure 7 (near Fermi edge region) clearly shows the increase in the high binding energy peak with respect to the low binding energy peak (which contains any metal intensity), which is consistent with an increase in the amount of high oxidation state (MoO_3 and perhaps Mo_2O_5) oxide. It is interesting to note that an increase in Mo_2O_5 with respect to MoO_2 would lead to a reduction in both the intensity and width of the low binding energy feature in the valence band (Figure 2), and the data in Figure 7 show a slight narrowing of the width of the low binding energy peak. The relative oxide-to-metal intensities in both the surface and bulk-sensitive regions are similar for both the core (Table 6) and valence band regions (Table 5), again indicating the homogeneous nature of the oxide film with depth.

Oxide Thickness, Type, and Electrochemical Significance. The behavior of the molybdenum metal upon electrochemical treatment at the given potentials represents an increase in the extent of oxidation with respect to an increase in the potential throughout the active region of molybdenum. As the active region is entered, oxide formation ensues. The extent of Mo(IV) and Mo(V/VI) formation increases with increasing potential. Also, the amount of formation of Mo(V/VI) increases above that of Mo(IV) as time increases.

If the oxide layer were a uniform oxide layer on top of the metal, then the approximate thicknesses of the oxide layer can be calculated using the usual inelastic electron energy loss model[34] to give the results in Table 7. The calculations of the thicknesses take into consideration the relative amounts of each oxide present on the surface of the metal, as given by the curve-fitting details (Table 4). The inelastic mean free path used in the model are calculated from the Seah and Dench equations[33−35] using an average oxide composition of MoO_2 and MoO_3. If this model were correct, then the values of the thickness of the oxide layer should be similar with respect to takeoff angle. Clearly the unreasonably small values at surface-sensitive angle show that this model is inappropriate. The only way to explain the small amounts of variation in composition with takeoff angle seen for many of the cases discussed above is that the film is reasonably homogeneous over the depth probed. Using the sine(takeoff angle) dependence expected and the inelastic mean free paths discussed above one would expect to get about 67% of the data from an approximately 19 Å layer for oxide species at bulk-sensitive angles, and from approximately 2 Å layer for oxide species in the case of surface-sensitive angles. This implies that the oxide film consists of a mixed layer of oxide species (Mo(IV) and Mo(V/VI)) rather than a layer with the higher oxidation state species (Mo(V/VI)) above the lower oxidation state species (Mo(IV)). The metal would also be present throughout this film. This means that the oxidation of molybdenum leads to a surface layer consisting of an oxidized film that contains a mixed layer with a range of oxidation states, which becomes mechanically unstable (see 2.0 V studies above) and falls off to expose the underlying metal.

Table 7. Approximate Thicknesses of the Adsorbed Metal Oxide Layers

sample treatment	50°, Å	5°, Å
as received		
polished	4.1	0.7
-0.5 V	3.2	0.4
0.0 V	4.0	0.5
0.5 V	32.8	3.3
1.0 V	29.7	3.4
1.5 V	28.3	3.9
2.0 V, 10 s	32.7	2.5
2.0 V, 30 s	43.4	4.2
2.0 V, 2 min	33.5	4.1

We find no experimental or theoretical evidence that MoO_2 should exist with two core Mo 3d binding energies as has been suggested earlier.[36] MoO_2 may often have some surface MoO_3 which would, of course, give additional high binding energy features in the Mo 3d region. The range of possible molybdenum oxidation states makes it difficult to conclusively determine this point experimentally since no preparation method can ensure only MoO_2 formation in the surface and bulk. Certainly the structure is a distorted rutile structure characterized by chains of edge-sharing MoO_6 octahedra with two different Mo−Mo distances (2.5 or 3.1 Å). The lower binding energy peak in the near Fermi-edge region (Figure 2) does indeed have Mo−Mo bonding character. However, there is only one Mo site in the crystal structure, and, as expected, our band structure calculation (which fully takes into account this crystal structure) predicts only a single Mo 3d feature (with the expected small amount of dispersion in the band for this core level). Our band structure calculations predict a separation between the Mo 3d binding energies of 1.06 eV between MoO_2 and Mo_2O_5 and 1.86 eV between Mo_2O_5 and MoO_3 compared to 1.5 and 1.4 eV found experimentally. Earlier workers have suggested[36] that

(36) Brox, B.; Olefjord, I. *Surf. Interface Anal.* **1988**, *13*, 3.

final state effects might give two peaks. We cannot exclude this, but find no evidence for such an effect, and there is certainly nothing special about the structure of MoO_2 that would lead one to look for such an unusual feature in a structure with only a single Mo site.

Conclusions

The work presented in this paper shows how core XPS data are interpreted by curve fitting and how valence band XPS interpreted by spectra generated from band structure calculations can provide complementary information in the investigation of molybdenum electrochemical oxidation. It is important to try to achieve complementary information, as curve fitting, when inappropriately carried out, can lead to significant error in interpretation especially when (as in this case) there are many possible oxidation products present. The results are consistent with the formation of both Mo(IV) and Mo(VI), and/or some intermediate oxidation state oxide including Mo(V) in some cases, on the molybdenum metal surface upon application of potentials within the active range of molybdenum in 0.5 M H_2SO_4. The oxide film becomes mechanically unstable and can fall off to reveal underlying metal when the oxidation is performed at highly anodic potentials for longer time periods.

Acknowledgment. The material is based upon work supported by the National Science Foundation under Grant No. CHE-9421068.

CM960187M